Version of Record: https://www.sciencedirect.com/science/article/pii/S2352492821006619
Manuscript_4eb6ec5abf727201101c3c66a4c8da16

Improvement of interfacial adhesion of unidirectional textile grade carbon fiber (TCF) with unsized, epoxy and urethane sizing reinforced in thermoset urethane composites

Surbhi Kore[a], Merlin Theodore [c,d], Renjith Pillai[e], Vinoy Thomas[e] and Uday Vaidya [a,b,c]

a. *Tickle College of Engineering, University of Tennessee, Knoxville, TN, USA;*

b. *Institute for Advanced Composites Manufacturing Innovation (IACMI), Knoxville, TN, USA*

c. *Energy and Transportation Sciences Division, Oak Ridge National Laboratory, Oak Ridge, TN, USA*

d. *Carbon Fiber Technology Facility, Oak Ridge National Laboratory, Oak Ridge, TN, USA*

e. *Materials Science & Engineering, University of Alabama, Birmingham, AL, USA*

**Corresponding author:*

Tel: +1-865-974-7620

E-mail: uvaidya@utk.edu

Abstract

This work considers a unique wide tow (450k filaments) form of low-cost carbon fiber intended for non-aerospace applications. TCF is currently produced in epoxy and urethane sizing, and there is a need to understand its resulting composite properties. In this study, the interfacial adhesion of sized TCF reinforced in thermoset urethane (TSU) composites are examined through the surface, thermal and mechanical characterization techniques. Atomic force microscopy (AFM) results showed an increase in surface roughness for urethane (276%) and epoxy sized (78%) versus unsized TCF. XPS results showed 531% increase in O in epoxy sized TCF and 250% N content in urethane sized TCF compared to unsized TCF. The surface energy of epoxy and urethane sized TCF is enhanced by 78% and 96%, respectively compared to unsized TCF. The storage modulus showed improvement for urethane (23%) and epoxy (21%) sized than unsized TCF-TSU composites. The flexural, interlaminar shear strength (ILSS), and impact properties of urethane sized TCF increase by 24%, 50%, and 273%, respectively, than unsized TCF. The results demonstrate that the surface and thermal properties correlate with the mechanical properties of TCF-TSU composites and sizing enhances the wettability of the composites.

© 2021 published by Elsevier. This manuscript is made available under the Elsevier user license
https://www.elsevier.com/open-access/userlicense/1.0/

Keywords: Textile grade carbon fiber (TCF), epoxy sizing (TCF-E), urethane sizing (TCF-U), unsized (TCF-UN), surface, thermal and mechanical properties

1. Introduction

Polyurethane (PU) is one of the versatile material due to its broad chemical structure leading to its thermoplastic, thermoset, and bio-based forms. The broad classification provides the combination of durability, stiffness, and flexibility, high impact strength, corrosion resistance compared to metals [1], [2]. The diversity in physical and chemical properties increases its usage in coatings, adhesives, fibers, foams, elastomer and composites [3–5]. However, PU has several drawbacks such as poor thermal stability, low processability low stiffness, and strength [6]. Hence various fillers (carbon nanotubes, metal oxides [7–10]) and fibers (glass [11], carbon (CF), natural fibers [12,13]) are incorporated into the urethane matrix to improve the strength of the material [7]. Among several fillers and fibers, the CF usage has increased greatly in structural and functional applications due to its properties such as high strength, stiffness, low density, chemical and heat resistance, and corrosion resistance [14,15]. The high-performance of carbon fiber attribute has drawn significant attention in automotive, aerospace, marine, sports, and other fields [16,17]. However, the performance of carbon fiber reinforced polymer composites (CFRP) depends on the interatomic and intermolecular contact between the fiber and matrix at the interface that impacts adhesion. The adhesion efficiency of CF can be modified using several surface treatment techniques such as liquid oxidation, gaseous oxidation, plasma oxidation, electrochemical oxidation, surface grafting, and polymer sizing [18]. Polymer sizing has become a promising method because it can bound to the CF surface by developing chemical groups compatible to the polymer matrix.

Gnadinger et al. [19] studied the interfacial shear strength of epoxy, urethane and PA sized CF with thermosetting urethane and epoxy matrices. A significant improvement (50%) in the IFSS properties was observed for the similar chemical structure of sizing agent and polymer. Zhang et al. [20] modified

CF surface by grafting MDI to understand the interfacial adhesion between CF and thermoplastic polyurethane (TPU). The author observed improvement in the tensile properties by 99% and thermal and microscopy results coordinate with mechanical properties of CF-TPU composites. Zhao et al.[21] improved the interfacial bonding by applying polydimethylsiloxane bishydroxylalkyl (PDMSBH) on CF surface and reinforced in PU matrix. The results indicate improvement in the mechanical as well as friction and wear properties of the composite.

Prior studies confirm that sizing roughens the CF surface for chemical and mechanical interaction with matrix, thus contribute to improving the mechanical properties of the composite [22–24]. Most of the PU research has been conducted using CNT, natural fibers, and short CF reinforcement [12,25], however, there is limited reported research on surface treated TCF.

In this study, unidirectional TCF fiber with unsized, epoxy, and urethane sizing has been investigated. TCF (also referred to as 'low-cost carbon fiber') has been developed by at the Carbon Fiber Technology Facility (CFTF), Oak Ridge National Laboratory (ORNL), Oak Ridge, Tennessee, USA [21]. TCF is a low molecular weight (100,000 to 200,000 g/mol) PAN precursor-based CF, a wide tow (102 mm-127 mm width) fiber with 300-450 K filaments and explicitly designed for non-aerospace applications. TCF has potential in stiffness (modulus) driven applications in automotive, sporting goods, and industrial applications.

This work aims to study the physicochemical interactions of unsized, epoxy and urethane sized TCF reinforced in thermoset polyurethane (TSU). The change in surface morphology was measured using X-ray photoelectron spectroscopy (XPS) and atomic force microscopy (AFM). The morphological effect on the thermal and mechanical properties was examined through dynamic mechanical analysis (DMA), flexural, interlaminar shear strength (ILSS), and impact strength of the composites. The failure modes and bonding mechanism were investigated using scanning electron microscopy (SEM). The influence of sizing chemistry on the interfacial adhesion of TCF-TSU composites was evaluated.

2. Experimental

2.1 **Materials**

Polyether based TSU resin (Shore hardness 80D) was supplied by Huntsman Corporation, Texas, details are presented in Table 1. The unsized, epoxy and urethane sized TCF spools were provided by CFTF, ORNL, presented in Table.1, and corresponding nomenclature is summarized in Table 2. TCF-UN and TCF-U were obtained in a tow form. TCF-E was received as C-ply. Chomarat, Williamston, South Carolina, USA converts TCF spools into a non-woven fabric called C-ply (NCF, $[+45/-45]_{8S}$ fiber orientation, 240 gsm). The tow size of individual spool was 450K filaments and the sizing concentration on the TCF-E and TCF-U surface was 1% and 2% by weight, respectively.

Table 1. Physical properties of TCF and TSU material [26]

Material	Density (g/cc)	Tensile strength (MPa)	Tensile Modulus (GPa)
TSU	1.23	89.8	3.15
TCF	1.77	3000	275

Table 2. TCF sizing nomenclature

Abbreviation	Sizing nomenclature	Sizing concentration
TCF-UN	Unsized TCF	NA
TCF-E	Epoxy sized TCF	1%
TCF-U	Urethane sized TCF	2%

2.2 **Methods**

Fabrication of TCF-TSU using hand-layup technique

TCF-E, TCF-U, and TCF-UN reinforced TSU laminate was fabricated using hand-layup method followed by a compression molding technique to achieve 60% fiber volume fraction consolidated panels. TSU (3:1 resin to hardener ratio) was stir for 10 mins to achieve the homogenous mixture of the component. The resin was spread on fourteen layers of TCF fabrics with C-ply (TCF-E) and tow bundle (TCF-U and TCF-UN), which was laid in a symmetric laminate sequence $[0, 90]_{7S}$. A perforated release

film (peel ply) was placed on the top of the fabric lay-up, and the entire setup was sealed with nylon 6 high temperature bagging material to absorb excess resin. The assembly was placed in a Carver hot press (Model 3895-compression molding press) which has 305 mm × 305 mm (12″ x12″) heated platens operated at 180 °C, and 0.6 MPa (83 Psi) to achieve 50-60 wt. % fraction of TCF-TSU composite.

Chemical reaction hypothesis:

The primary purpose of using epoxy and urethane sizing is because both are commercially available and have an active functional group which can readily react with hydrogen atom from primary/ secondary amine of TSU through nucleophilic addition reaction with epoxy sizing and trans-urethanization reaction with urethane sizing to improve the interface of the composites, presented in Figure 1.

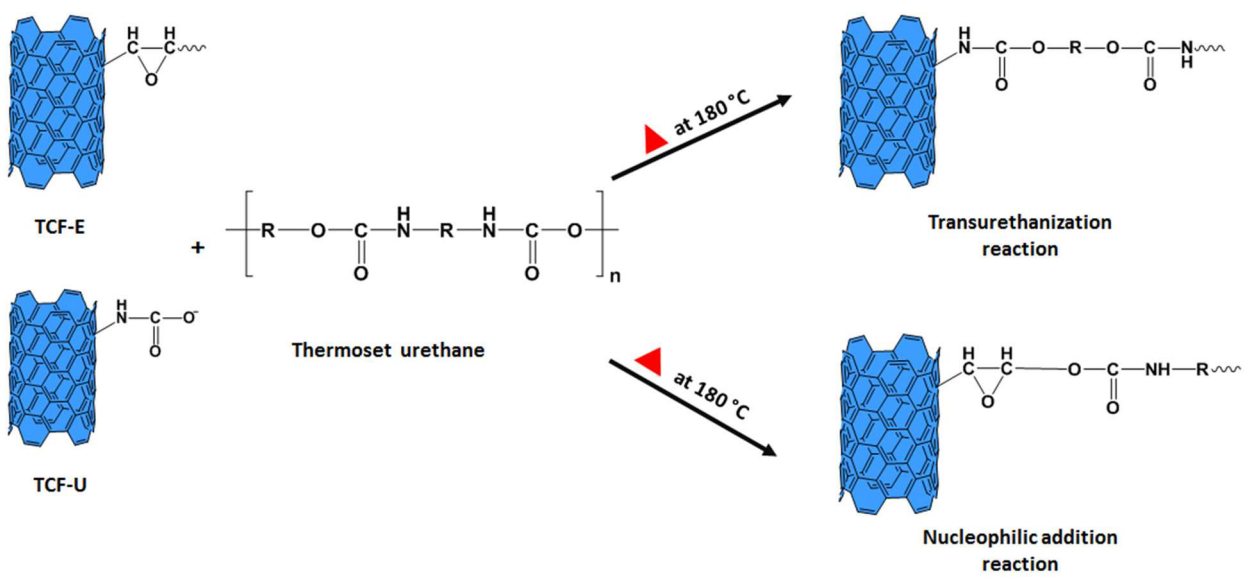

Figure 1. Possible chemical reaction at the interface of TCF-E and TCF-U with TSU matrix at 180 °C curing temperature [27,28]

Characterization techniques:

2.2.1 Atomic force microscopy (AFM)

AFM was used to understand the surface physical structure of TCF-UN, TCF-E, and TCF-U to evaluate the surface roughness. The MFD-3D infinity microscope (Oxford instrument, United Kingdom) with

AC/Air topography mode (JIAM, UTK, TN, USA) was used to produce 3D images. A monolithic cantilever (AC240TS-R3 from Oxford instruments) with force constant of 2 N/m and a resonance frequency of 70 kHz was used with tapping mode. The fiber tow was mounted on the glass slab using a double-sided tape. The scanning area was 20 μm× 20 μm at the scanning rate 1 Hz. The mean roughness (nm) and root-mean-squared roughness (RMS) values of unsized, epoxy and urethane sized TCF was determine using Gwyddion 2.55 (2019) version software.

2.2.2 *X*-ray photo-electron microscopy (XPS)

XPS techniques were used to determine the chemical composition and surface properties of TCF-UN, TCF-E and TCF-U. The characterization was performed using the Thermo Scientific Model K-alpha XPS instrument (at ORNL, Oak Ridge, Tennessee). A single point analysis was used with 400 μm diameter X-ray spot due to small size (7μm diameter) of fiber filament. All the spectra were collected by Al Kα X-rays (1486.6 eV) source, and a hemispherical electron energy analyzer equipped with a 128 multi-channel electron detection system operated at $2x10^{-9}$ mbar.

2.2.3 Dynamic mechanical analysis (DMA)

The dynamic mechanical analysis (DMA) was performed using Thermal Analysis (Q800, DE, USA) instrument on TSU using ASTM D-4064 [29], and for TCF-UN-TSU, TCF-E-TSU, and TCF-U-TSU composites using ASTM D 7028-07 [30]. The storage modulus, loss modulus, and tan δ were measured as a function of temperature from -100–250°C at 5°C/ min. Tests were performed using a three-point bending device with a dual cantilever mode at an operating frequency of 0.5 Hz for polymer and 1 Hz for composites.

2.2.4 Thermogravimetric analysis (TGA)

TGA was performed on TCF-UN-TSU, TCF-E-TSU, and TCF-U-TSU composites to understand the degradation behavior and weight loss with respect to temperature, using a TGA Q50 Thermogravimetric analyzer (TA instrument, DE, USA). All the characterization was performed under nitrogen atmosphere and temperature ramped from 25 °C to 800 °C with a heating rate of 20 °C/ min.

2.2.5 Contact angle measurement

The surface wettability of TCF-Un, TCF-E, TCF-U, and TSU resin was measured using the sessile drop method [31] at room temperature with a Glycerol (γd = 34 mN/m, γp = 30 mN/m) as a single liquid system. The size of the liquid droplet was 5 µL. The measurement was aided by the Image J software, and video based contact angle instrument and software (VHX 600E, Keyence). Six specimens were tested per sample by mounting the fiber and matrix on a glass slab, and the surface energy was evaluated by thermodynamic model of adhesion with Antonov's empirical rule. Equations 1 represents contact angle where Θ = equilibrium contact angle; γ_S = surface energy of solid (mN/m); and γ_L= surface energy of the liquid (mN/m) [32].

$$Cos\ \Theta = \frac{2\gamma_S}{\gamma_L} - 1 \ldots\ldots\ldots\ldots\ (1)$$

2.2.6 Flexural testing

The flexural test was performed on the TCF-TSU panels according to ASTM D790-17 [33]. A three-point bend test fixture was used on the Test Resources Universal Testing Machine (UTM) machine (Model 313 series frame, MN) with a 50 kN load cell. Five specimens were tested for each configuration with the dimensions of 65mm × 12.7 mm × t. The crosshead rate is in the range of 0.87 to 1.33 mm/minute.

2.2.7 Interlaminar shear strength (ILSS)

The interlaminar shear strength test was conducted on TCF-TSU composite according to ASTM D-2344 [34]. Five specimens were tested with a crosshead rate of 1 mm/minute on the Test Resources Universal Testing Machine (UTM) machine (Model 313 series frame, MN) with a 50 kN load cell.

2.2.8 Impact strength testing

The IZOD impact characterization was performed to understand the effect of interfacial bonding on the absorption capacity of TCF-TSU composites. Five specimens for each material with dimensions 65mm × 12.7mm × 2.5-3 mm was prepared using a notch type A with a radius of 0.25 mm and notch angle of

45° according to ASTM D-256 [35]. The specimens were tested using the Tinius Olsen (Model IT 504, PA, USA) machine with a pendulum weight of 37 N and 22.6 J loading capacity. The average impact strength was calculated and reported.

2.2.9 Scanning electron microscopy (SEM)

Zeiss Auriga electron microscope was performed on the fracture surfaces of TCF-TSU composites to evaluate the bonding mechanism. The fractured samples were coated with gold (SPI-MODULE^{TM} sputter coater, PA, USA) for 30 sec to improve the resolution of the micrographs. SEM was operated at 5 kV to characterize the interfacial adhesion of TCF surface.

3. Results and Discussion

Surface Characterization of sized and unsized fibers

3.1 Atomic force microscopy (AFM)

AFM was used to evaluate the surface morphology of unsized and sized TCF at nanoscale to identify the surface roughness of CF. Figure 2 shows the presence of extended grooves along the axial direction of the unsized fiber surface [36]. After sizing, the change in the surface structure of TCF is observed through height v/s distance plot created by measuring the depth of the groove and width profile. The surface roughness values are presented in Table 3. The grooves depth and width on the fiber surface, i.e., the spiked region in Z-direction was analyzed using Gwyddion 2.55 (2019) version software.

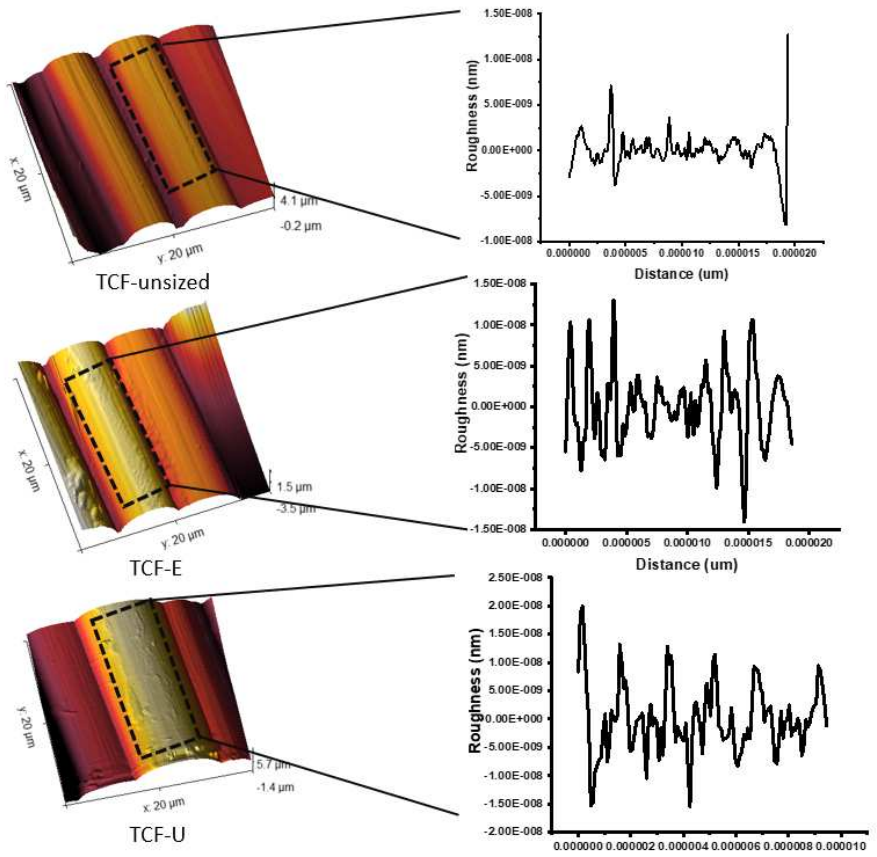

Figure.2 Three-dimensional AFM images of unsized (TCF-UN), epoxy sized (TCF-E) and urethane sized (TCF-U) CF with its surface roughness profile image in Z-direction. The surface roughness increases from TCF-UN<TCF-E<TCF-U

Table 3. Surface roughness of TCF-UN, TCF-E, TCF-U

Specimens	Mean roughness (nm)	Root mean square roughness (nm)
TCF-UN	120.2	163.1
TCF-E	228.6	291.9
TCF-U	457.6	612.6

The sizing changed the surface topography by reducing the groove structure on the TCF surface. The AFM images of TCF-UN show a smooth surface, and after the addition of a 1% concentration of epoxy sizing, the surface roughness improved by 78% from 163.1nm (TCF-UN) to 291.9 nm (TCF-E). The

non-uniform distribution of epoxy sizing was observed on the surface roughness profile, which may provide a different effect on mechanical interlocking [37]. The TCF-U contains a 2% sizing concentration enhances the surface roughness by 276% from 163.1 nm (TCF-UN) to 612.6 nm (TCF-U). The roughness profiles reveal no evidence of groove structure indicates the uniform distribution of sizing on the fiber surface. The interfacial adhesion between fiber and matrix depends on the surface roughness values. As the sizing concentration increases, it enhances the number of sites (increases surface roughness) for mechanical interlocking, which hypothesized to increase the overall strength of the composites. The results show that TCF-U has higher surface roughness values compared to TCF-E and TCF-UN which interpret to enhance the mechanical properties of the TCF-U-TSU composites than other constituent materials.

3.2 X-ray photo-electron spectroscopy (XPS):

XPS was performed to identify the chemical/surface composition of carbon (C 1s), oxygen (O 1s), and nitrogen (N 1s) on sized TCF. The survey spectra of individual constituents are presented in Figure. 3 and Figure 4, respectively. The reactive components of TCF-U and TCF-E are -NHCOO- and oxirane ring (O-C-O). The atomic concentrations of TCF-UN, TCF-E and TCF-U are presented in Table 4. The XPS peaks for TCF-E shows the presence of C-C (284.4 eV), C-O-C (289.1 eV), C-O (289.1 eV), and C=O (532 eV) groups, and for TCF-U, C-C (284.4 eV), C=O (285.1 eV), CH_2 (285.7 eV), C-N (286.5 eV), O-CH (289.1 eV), O=C-O, C=O (531.8 eV), C-O (533.2 eV), and N-H (399.9 eV) groups.

The concentration of C decreased by 16% after the addition of sizing on TCF surface by producing molecular linkages. TCF-E (19.6) showed higher oxygen content compared to TCF-UN (3.1) and TCF-U (15) due to the presence of oxirane ring from epoxy sizing. The TCF-E (0.24) and TCF-UN (1.0) showed a small amount of nitrogen content, which we hypothesize developed during the carbonization and oxidization process. The TCF-U contains higher N content (250% higher than TCF-UN) which contributed to the presence of amine in urethane sizing. The results confirm the presence of epoxy and urethane groups on the TCF surface.

As compared to the reactivity of both the sizing, oxirane ring contain secondary hydroxyl group which has a less reactivity compared to amine group from urethane linkage, when reacting to isocyanates from TSU, presented in Figure 1. Hence, it can be interpreted that TCF-U can form a strong hydrogen bond with TSU (due to similar molecular structure) compared to TCF-E. The presence of strong polar groups on the TCF-U surface can enhance its interfacial bonding with TSU compared to TCF-E. This data is aligned with AFM results and illustrates that the polarity of the sized component enhances the surface roughness of TCF.

Table 4. Chemical composition and atomic ratio of epoxy and urethane sized and unsized TCF

Surface Composition (at. %)	C	O	N	C/O	C/N
TCF-UN	95.7	3.1	1.0	30.87	NA
TCF-E	79.81	19.57	0.24	4.1	NA
TCF-U	81.3	15	3.5	5.42	23.2

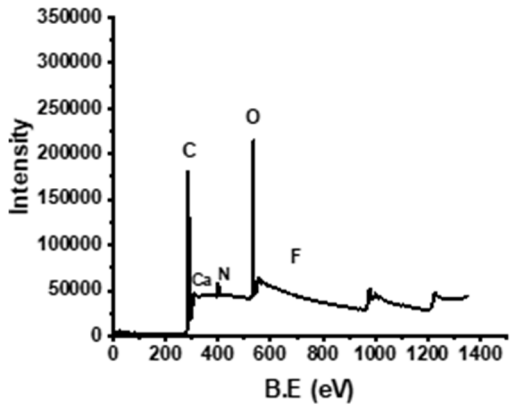

(a)

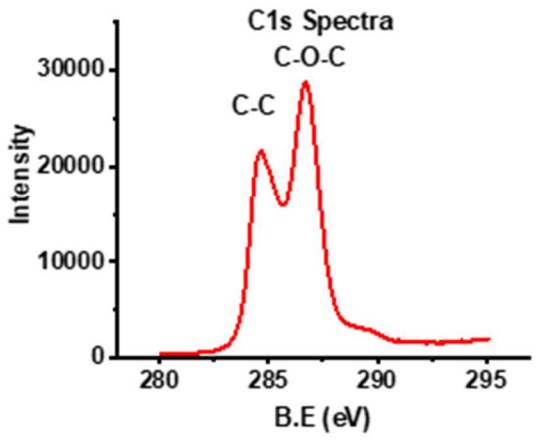

(b)

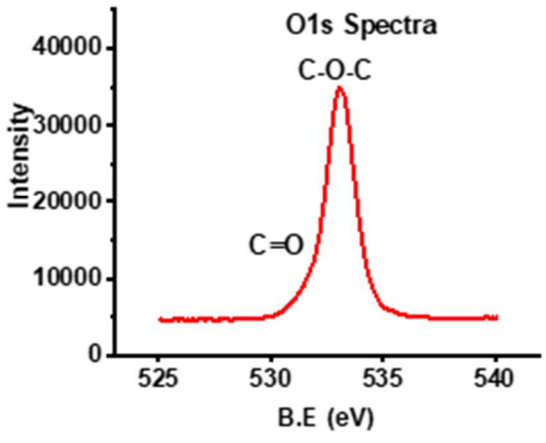

(c)

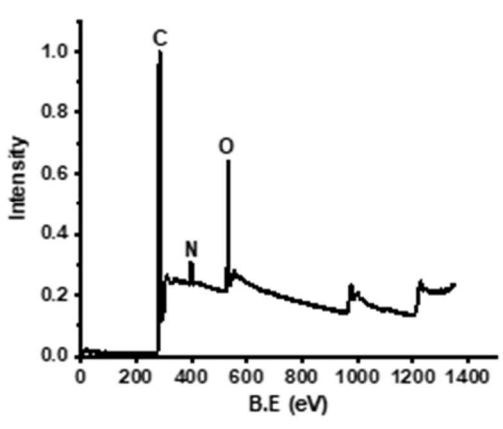

(a)

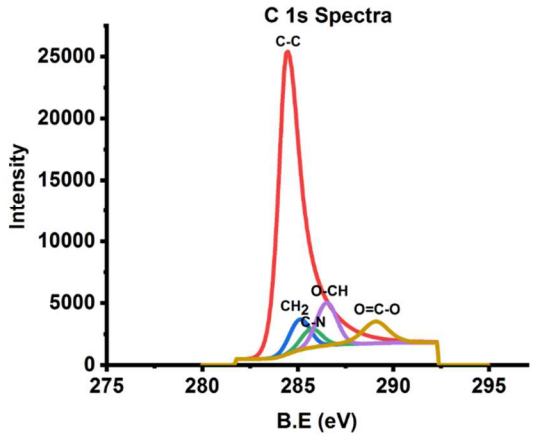

(b)

Figure. 3 (a) XPS survey spectra of TCF-E shows higher concentration of C and O elements, (b) C 1s spectra shows C-C bond from TCF structure and C-O-C from sizing, (c) O 1s spectra shows the presence of oxirane structure (C-O-C) from epoxy sizing.

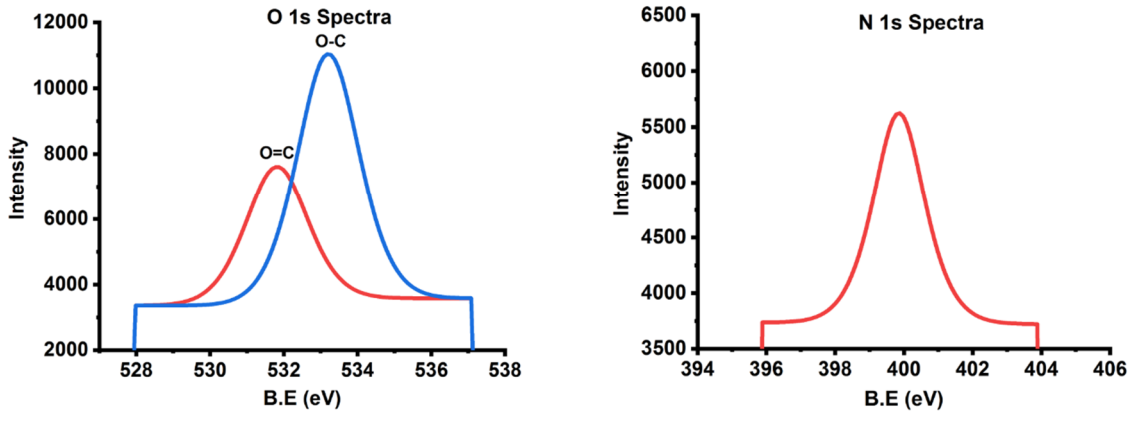

(c) (d)

Figure.4 (a) XPS survey spectra of TCF-U shows higher concentration of C, O and N elements, (b) C 1s spectra shows C-C from TCF structure, (c) O 1s spectra shows C-O and C=O and (d) N 1s spectra shows NH group (NHCOO) structure from urethane sizing.

3.3 Contact angle measurement

The surface energy of TCF-Un, TCF-E, TCF-U, and TSU resin was calculated using Antonov's equation explained in Section 2.2.5 and the data is presented in Table 5. TCF-Un showed the lowest surface energy (25.01 mN/m) due to lack of functional group(s) on the TCF surface. Both epoxy and urethane-sized TCF exhibited 78% and 96% improvement in surface energy. The difference in the data was mainly contributed to the reactivity of epoxy (C=O) and urethane linkage (COONH) (as explained in Section 3.2). Jiao et al.[38] observed a similar trend, and stated that the polarity of the functional group enhances the surface energy of CF due to the sizing chemistry. The data coincides with the AFM results inferring that the polarity of sizing influences the surface roughness of TCF. The surface energy of TCF-U (49 mN/m) is similar to TSU resin (≈48 mN/m); hence it can be concluded that TSU will provide strong wettability with TCF-U along with strong interfacial bonding and hence will enhance the mechanical properties of the TCF-U-TSU composites than TCF-E-TSU and TCF-Un-TSU.

Table 5. Surface energy and contact angle measurement results of sized TCF fiber and TSU resin

Component	Contact angle (°)	Surface energy (mN/m)
TSU (resin)	60.88 ± 2.2	47.57
TCF-UN	102.61 ± 5.9	25.01
TCF-E	66.95 ± 7.7	44.53
TCF-U	57.69 ± 1.3	49.10

*All the tested data measured using sessile drop test.

Thermal characterization of TCF-TSU composites

3.4 Thermogravimetric analysis (TGA)

Thermal stability, fiber content, and decomposition temperature have been analyzed using TGA under a nitrogen atmosphere. Normalized TGA curves of epoxy, urethane and unsized TCF are presented in Figure. 5 and the percentage of weight loss data was studied. The unsized, epoxy, and urethane-sized TCF composites showed similar decomposition trends with one stage of weight loss, and the transition starts at the 215-300°C and the final transition observed at 600°C. During the thermal transition of TCF-TSU composites, three minor degradation steps were observed. The first step observed at 305-358 °C, indicates the separation of polyol and isocyanate; the second and third step obtained in the range of 374-550°C implies the formation of carbon dioxide [39]. The percentage weight loss for TCF-UN, TCF-E, and TCF-U composites is 59%, 68%, and 76%, respectively.

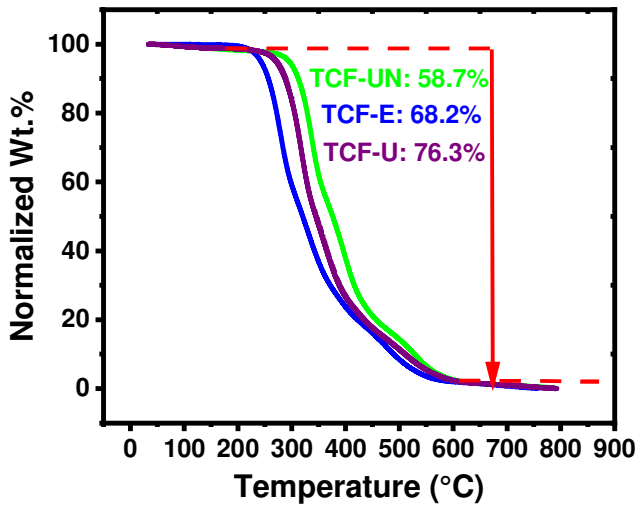

Figure. 5 Normalized TGA curves of different sized TCF reinforced in TSU composites, (a) 59% fiber wt. fraction in TCF-UN, (b) 68% fiber wt. Fraction in TCF-E, (c) 76% fiber wt. Fraction in TCF-U

The difference in the fiber volume fraction is attributed due to the difference in the sizing concentration. Wang et al. [40]stated that the high fiber content enhances the mechanical strength and modulus of composite by restricting the molecular movement of the polymer through a strong hydrogen bonding network between fiber and matrix. The results interpret that TCF-U can provide higher (due to an increase in 12% and 29% fiber content than TCF-E and TCF-UN, respectively) mechanical properties of the composites than TCF-E and TCF-UN.

3.5 Dynamic mechanical analysis (DMA)

DMA was performed on unidirectional TCF-TSU composites specimens to evaluate the elastic stiffness and energy dissipation capacity of composites as a function of temperature. The variation of storage modulus (E') and tan δ curve as a function of temperature are presented in Figure 6. Keusch et al [41] stated that storage modulus is directly, and tan δ is inversely proportional to interfacial bonding of composites. The difference in the initial storage modulus (at –100 °C) after incorporating sized TCF indicates an improvement in the interfacial bonding of composites, Figure 6(a). As shown in Table.5, compared to TSU, the E' results of unsized, epoxy sized, and urethane sized TCF increases by 632.7%,

785.3%, and 800.0%, respectively. However, Edie et al [42] reported that the fiber volume fraction (V_f) significantly affects the E´ value. Hence the damping factor curve was analyzed to understand molecular motion at the interface and quantifies the interfacial bonding of composite.

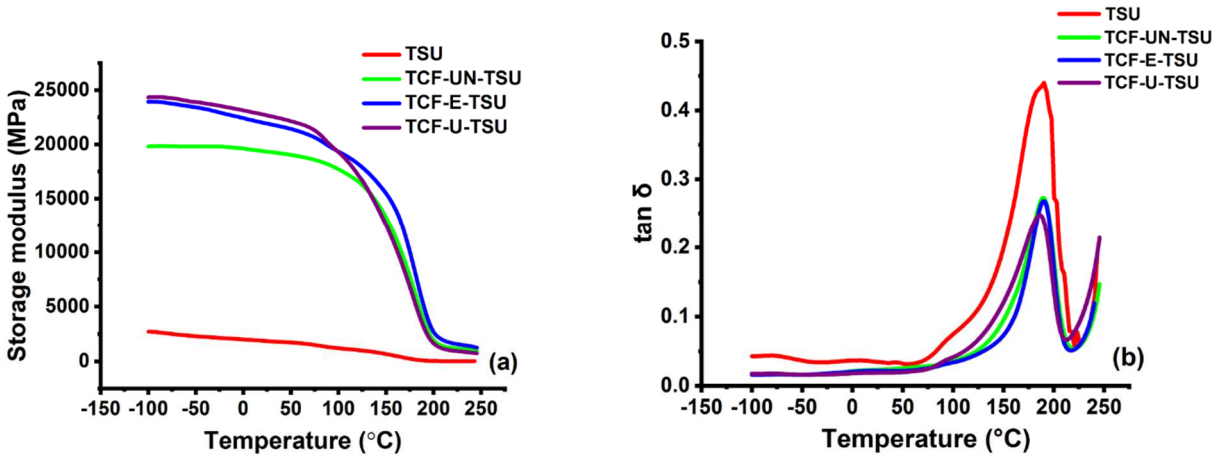

Figure 6. Dynamic mechanical characteristics of TSU (0.5 Hz) and TCF-TSU composites (at 1 Hz) with unsized, urethane and epoxy sizing on TCF surface: (a) the storage modulus, (b) damping factor (tan δ) as a function of temperature.

The tan δ curve of TCF-UN, TCF-E, TCF-U reinforced TSU composites are shown in Figure. 6(b). The peak temperature of the tan δ curve represents the glass transition temperature listed in Table.6. The Figure 6(b) showed no remarkable difference in the Tg value. However, the damping behavior at the Tg of TCF-UN and TCF-E was observed higher than TCF-U; the difference emphasizes poor interfacial bonding in TCF-E and TCF-UN composites. The tan δ values has decreased 2.2% from 0.2725 for TCF-UN to 0.2665 for TCF-E and 9.2% (0.2474) for TCF-U. A composite with strong interfacial bonding tends to restrict the motion of the molecular chain at the interface by providing less dissipation energy, which decreases the height of the tan δ peak [41]. Hence, urethane sized TCF composite has a strong interfacial bonding compared to epoxy and unsized TCF composite.

Table 6. Storage modulus (E'), tan δ and fiber volume fraction of TCF-TSU composites with epoxy and urethane sizing treatments

Material	E’ MPa (at -100°C)	Tan δ	V_f
TSU	2704.1	0.4347	-
TCF-UN-TSU	19813.1	0.2725	50
TCF-E-TSU	23938.2	0.2665	60
TCF-U-TSU	24337.1	0.2474	69

The AFM findings suggest that the urethane sizing increases the groove's depth on the TCF surface compared to epoxy sizing and thus increases the surface roughness that enhances the wettability of TCF-U with TSU resin. The polar groups present on the TCF-U surface (XPS results) can have good interface adhesion with TSU than TCF-E due to similar molecular structure. Thus, the increase in the molecular interaction in the fiber and matrix can produce a strong hydrogen bond that enhances the interfacial strength and the volume fraction of the composites and restrict the molecular mobility of TSU at the interface by decreasing the peak height of tan δ. The strong interface helps to transfer stress uniformly from fiber to matrix and provides excellent mechanical strength of the composites. Therefore, all the characterization interpret that TCF-U can provide excellent mechanical properties than TCF-E and TCF-UN.

Mechanical Characterization of TCF-TSU composites

3.6 Flexural properties:

Flexural properties of unsized, epoxy, and urethane sized TCF reinforced TSU composites are presented in Figure 7. Based on the surface analysis of AFM and XPS, it can infer that the surface roughness developed by the urethane (polar groups) sizing enhanced the flexural strength of TCF-U composites compared to TCF-E and TCF-UN. The flexural strength increases by 24% and 7% from 482 ± 25 MPa of TCF-UN to 598 ± 77 MPa of TCF-U and 515 ± 66 MPa of TCF-E. The enhancement in flexural strength indicates excellent interfacial adhesion between fiber and matrix due to chemical

interaction and reduces fiber separation from the matrix [43,44]. The strong interface between TCF-U and TSU might contributed to a hydrogen bond formation by a trans-urethanization reaction. In this reaction, the active functional group from sized TCF gets crosslinked with a reactive group of urethane polymer through intermolecular interaction. The hydrogen bond creates a bridge between fiber and matrix and enhances the flexural strength of the compounds [45,46]. Furthermore, the flexural strength of TCF-E is still higher than TCF-UN, either due to the mechanical interlocking or poor chemical interaction of epoxy and urethane linkages, which showed less increase in the properties. Flexural modulus is also presented in Figure. 7. The results showed a similar trend where TCF-U-TSU (58±6.2 GPa) has higher stiffness than TCF-E-TSU (50±1.2 GPa) and TCF-UN-TSU (38±1.2 GPa) composites. It can hence be inferred that that strong interfacial interaction increases failure resistance of composites [19].

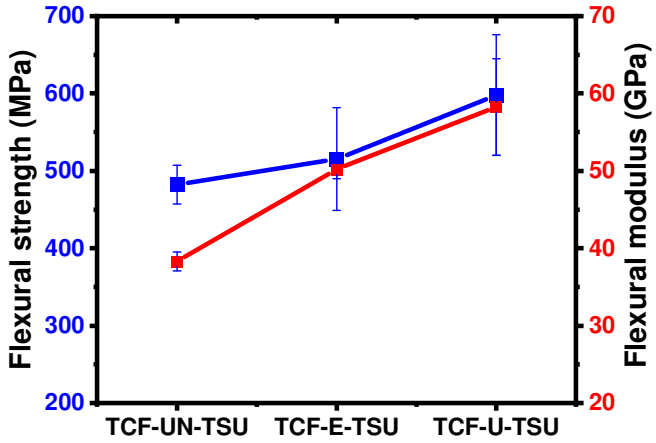

Figure 7. Flexural strength and modulus of unsized, epoxy and urethane sized TCF reinforced in TSU composites

3.7 Interlaminar Shear Strength (ILSS)

ILSS test was performed to understand the interfacial bonding between TCF-UN, TCF-E, and TCF-U with TSU polymer and the results compared with contact angle of each constituent presented in Figure 8. ILSS properties depend primarily on the matrix properties and fiber-matrix interfacial strength rather

than the fiber properties [47]. As shown in Figure 8, the ILSS results improved from 15 ± 0.9 MPa (TCF-UN) to 21.9 ± 3.7 MPa (TCF-E) (46%) due to epoxy sizing, which not only roughens the surface for mechanical interlocking, but also provides oxirane functional group to enhance the wettability between fiber and matrix. The TCF-U contributed largely to ILSS properties from 21.9 MPa to 32.09 ± 2.1 MPa with a 50% improvement. The data also showed an inversely proportional relation between contact angle and ILSS properties. Thus, the improvement in the strength confirms the presence of a chemical bridge between fiber and matrix that enhanced interfacial adhesion. This behavior of results is correlated with the flexural properties of TCF-TSU composites. The obtained ILSS properties are higher in comparison to CF-epoxy composite [48] and glass fiber- MWNT-epoxy hybrid [49] composites.

The typical stress-strain curve reveals the different failure patterns of TSU composites. The material did not show catastrophic failure due to the different segments of urethane. Two stages of failure were observed in ILSS for sized TCF composites. In the first stage, initial failure is achieved with maximum stress and transfer to the second stage. In the second stage, the crack induced with a slight decrease of load and propagated through the interface until it breaks completely. However, for unsized TCF, the ILSS curve breaks smoothly at the initial stage. Hence, the breakage illustrates that sizing protects crack transfer by enhancing fracture energy absorption capacity and effectively increasing interfacial bonding of urethane and epoxy sized composite.

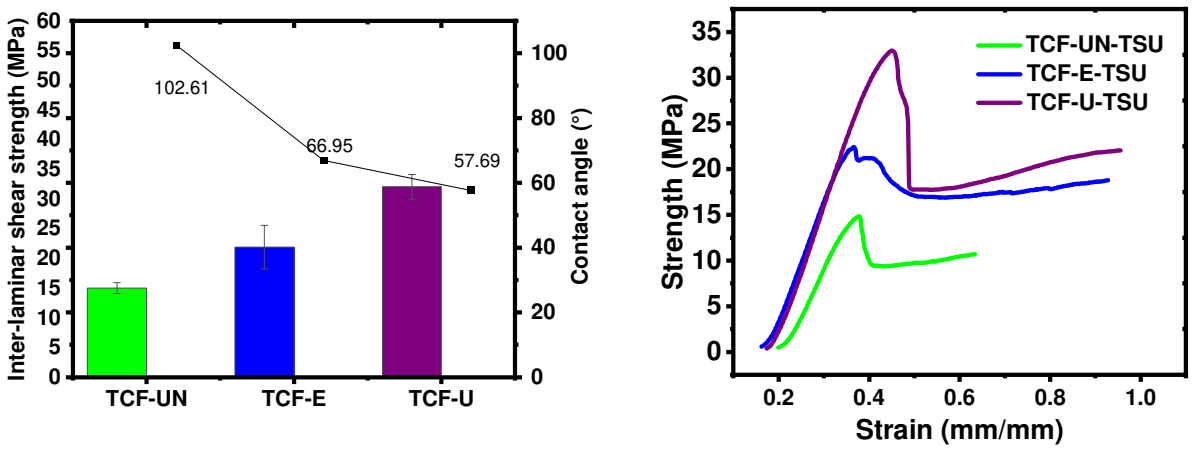

Figure 8. Interlaminar shear strength and typical stress strain curve of TCF-UN (15 MPa), TCF-E (21.9 MPa) and TCF-U (32.1 MPa) reinforced in TSU composites

3.8 Impact strength:

Impact strength is the capacity of a material to dissipate the energy applied at high-speed loading [50]. Figure. 9 shows the impact strength of TCF-UN, TCF-E, and TCF-U reinforced TSU composites. The trend of impact strength is consistent with flexural and ILSS properties. As shown in Figure 9, the impact strength results improved from 29.1 ± 4.5 J/m (TCF-UN) to 63.1 ± 2.8 J/m (TCF-E) (116%) by epoxy sizing. Similarly, the impact strength of TCF-U improved by 170% from 29.1 J/m to 78.6 ± 14.8 J/m.

The urethane sized significantly improved the toughness of the TCF reinforced composites by enhancing the interlocking efficiency at the fiber-matrix interface and allowed to increase the energy absorption capacity during impact loading [51]. Sizing provides efficient and effective resistance to crack propagation during impact loading due to strong interfacial adhesion in the composite.

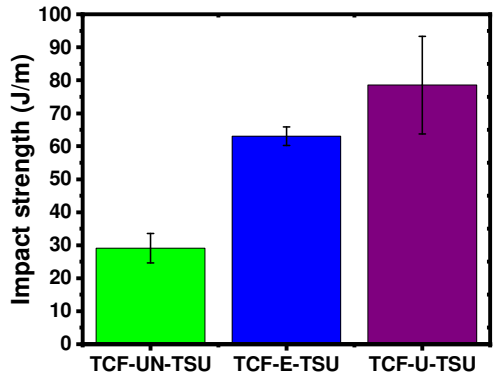

Figure 9. Izod impact strength of untreated (29.1 J/m), epoxy (63.1 J/m) and urethane sized (78.6 J/m) TCF-TSU composites

3.9 TCF's microstructure and surface morphology of fractured composites:

The SEM micrographs are performed on untreated, epoxy and urethane sized TCF to understand the interfacial interaction of TCF with TSU. The fractured images of the flexural test are presented in Figure 10 (a-c), respectively. The unsized TCF (Figure 10(a)) reveals a smooth surface with visible grooves parallel to the fiber axis. The micrographs also reveal less/no resin adhere to the TCF-UN surface, indicating the weak interface between fiber and matrix due to lower surface roughness (120 nm) that reduces the stress transfer from matrix to fiber, causing poor ILSS properties and eventually decreases the flex properties.

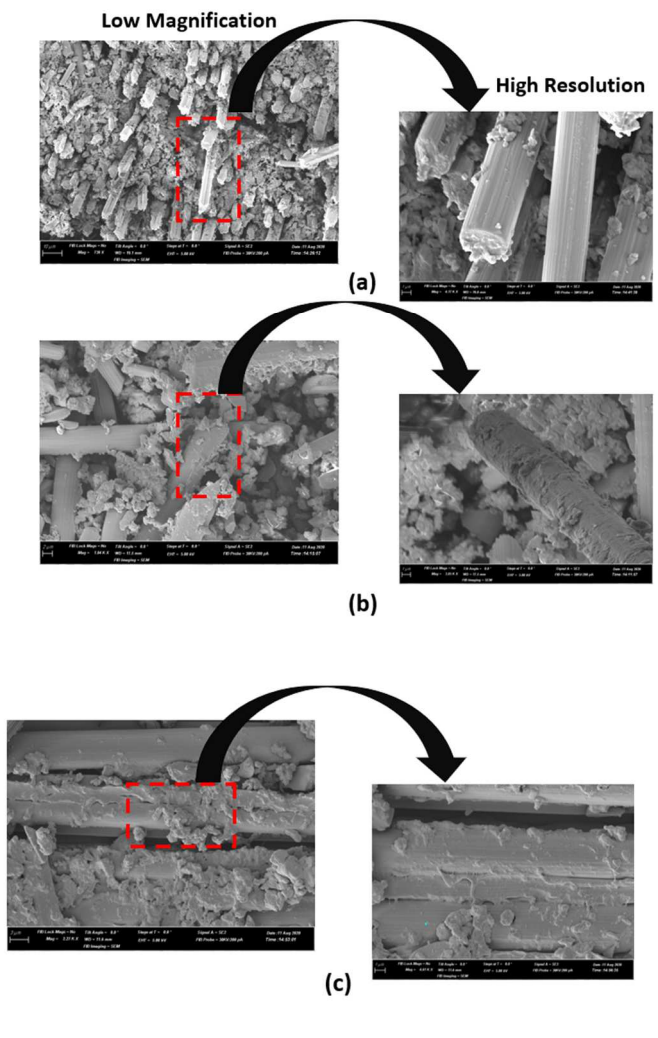

Figure 9. SEM micrographs of fracture surface morphologies for the TCF-TSU composites with epoxy, urethane and unsized surface sizing (a) TCF-UN-TSU, (b)TCF-E-TSU, (c) TCF-U-TSU at 4-10µm magnifications (left) and 1µm resolution (right).

Figure 9(b) shows the surface morphology of TCF-E, where a non-uniform coating of resin on the fiber was observed along with spindle size particles throughout the fiber length due to higher surface roughness (228.6 nm) compared to TCF-UN. This behavior develops a chemical/mechanical interaction between urethane and epoxy groups that improves the mechanical properties of TCF-E-TSU composite. While in Figure 9(c), a good fiber-matrix interaction was observed, and TCF-U has the highest surface roughness that is 457.6 nm, among other sized TCF that contributed to improved bond strength. Furthermore, the micrograph of TCF-U shows a homogeneous distribution of polymer on the fiber

surface that implies the crack induced during loading restrain the initial crack by absorbing intense energy. Additionally, sizing restricts the crack propagation and changes its direction by enhancing energy dissipation (DMA results) and provides the highest flexural and ILSS and impact properties in urethane sized TCF-TSU composite [15,52].

4. Conclusions

An efficient method was used to enhance TCF-TSU composite interfacial bonding through epoxy and urethane sizing on the TCF surface to evaluate the mechanical properties of the composites. It is observed from AFM and XPS characterization that TCF-U contains highly polar functional groups, which improves the surface roughness of TCF by providing 275% higher surface roughness compared to TCF-UN. The surface energy results using a glycerol liquid showed that TCF-U (49.1 mN/m) and TSU (47.57 mN/m) have similar surface energy values which can provide strong interfacial adhesion between fiber and matrix than TCF-E and TCF-Un. Compared to unsized TCF, the damping factor decreased by 9.2% and 2.2 % for composites. DMA results also reveal that TCF-U has a strong interface compared to TCF-E due to the similar molecular structure of TSU. Flexural and ILSS properties TCF-U-TSU composites enhanced by 24% (from 482±25 MPa to 515±66 MPa) and 50% (from 21.9±0.9 MPa to 32.09±2.1 MPa), TCF-U and TCF-E, respectively, suggesting better interfacial adhesion between TCF-U-TSU respectively, compared to TCF-UN-TSU. AFM, XPS, DMA, contact angle, mechanical properties, and fractured micrographs correlated to each other, suggesting better interfacial adhesion of TCF-TSU composites using urethane sizing. TGA data reveals that the TCF-TSU composite can withstand to 215°C, which can benefit high-temperature automotive applications. Hence, modifying the surfaces enhances the mechanical interlocking and chemical bonding and increases the efficiency of stress absorption through the interface by providing improved mechanical properties of the TCF-TSU composites. The overall structure of the work can be easily implemented in the production of cost-effective large-scale automotive applications.

Acknowledgement

This work was supported by the by the Office of Energy Efficiency and Renewable Energy (EERE), U.S. Department of Energy [grant numbers DE-EE0006926], the Institute of Advanced Composites Manufacturing Innovation (IACMI) and the Carbon Fiber Technology Facility (CFTF), Oak Ridge National Laboratory (ORNL), TN, USA, for financial and facilities support, respectively. We gratefully acknowledge part of the graduate student support for this work funded by Grant # P42 ES027723-01A1 from the National Institute of Environmental Health Sciences (NIEHS). Chomarat North America for the non-crimped weaving of the TCF is acknowledged.

Data Availability

The raw/processed data required to reproduce these findings cannot be shared at this time as the data also forms part of an ongoing study.

References

[1] J.O. Akindoyo, M. Beg, S. Ghazali, M.R. Islam, N. Jeyaratnam, A.R. Yuvaraj, Polyurethane types, synthesis and applications--a review, Rsc Adv. 6 (2016) 114453–114482.

[2] Z. Liu, G. Bai, Y. Huang, Y. Ma, F. Du, F. Li, T. Guo, Y. Chen, Reflection and absorption contributions to the electromagnetic interference shielding of single-walled carbon nanotube/polyurethane composites, Carbon N Y. 45 (2007) 821–827.

[3] G.W. Becker, D. Braun, G. Oertel, Polyurethane Kunststoff Handbuch 7, Carl Hanser. (1993).

[4] K.C. Frisch, Recent developments in urethane elastomers and reaction injection molded (RIM) elastomers, Rubber Chem Technol. 53 (1980) 126–140.

[5] G. Holden, Applications of thermoplastic elastomers, Carl Hanser Verlag, Thermoplast Elastomers a Compr Rev. (1987) 481–506.

[6] P.K. Prabhakar, S. Raj, P.R. Anuradha, S.N. Sawant, M. Doble, Biocompatibility studies on polyaniline and polyaniline--silver nanoparticle coated polyurethane composite, Colloids Surfaces B Biointerfaces. 86 (2011) 146–153.

[7] R.C.R. Nunes, J.L.C. Fonseca, M.R. Pereira, Polymer--filler interactions and mechanical

properties of a polyurethane elastomer, Polym Test. 19 (2000) 93–103.

[8] O.E. Otterstedt, J.-E. Otterstedt, J. Ekdahl, J. Backman, C.-H. Andersson, Fine colloidal silica as reinforcing filler in polyurethane polymers, J Appl Polym Sci. 34 (1987) 2575–2582.

[9] D. Feldman, M.A. Lacasse, Polymer--filler interaction in polyurethane kraft lignin polyblends, J Appl Polym Sci. 51 (1994) 701–709.

[10] J. Xiong, Z. Zheng, X. Qin, M. Li, H. Li, X. Wang, The thermal and mechanical properties of a polyurethane/multi-walled carbon nanotube composite, Carbon N Y. 44 (2006) 2701–2707.

[11] J. Nicholas, M. Mohamed, G.S. Dhaliwal, S. Anandan, K. Chandrashekhara, Effects of accelerated environmental aging on glass fiber reinforced thermoset polyurethane composites, Compos Part B Eng. 94 (2016) 370–378.

[12] A. Atiqah, M. T Mastura, B. A Ahmed Ali, M. Jawaid, S. M Sapuan, A review on polyurethane and its polymer composites, Curr Org Synth. 14 (2017) 233–248.

[13] R. V Silva, D. Spinelli, W.W. Bose Filho, S.C. Neto, G.O. Chierice, J.R. Tarpani, Fracture toughness of natural fibers/castor oil polyurethane composites, Compos Sci Technol. 66 (2006) 1328–1335.

[14] L. Hao, P. Peng, F. Yang, B. Zhang, J. Zhang, X. Lu, W. Jiao, W. Liu, R. Wang, X. He, Study of structure--mechanical heterogeneity of polyacrylonitrile-based carbon fiber monofilament by plasma etching-assisted radius profiling, Carbon N Y. 114 (2017) 317–323.

[15] M. Andideh, M. Esfandeh, Effect of surface modification of electrochemically oxidized carbon fibers by grafting hydroxyl and amine functionalized hyperbranched polyurethanes on interlaminar shear strength of epoxy composites, Carbon N Y. 123 (2017) 233–242.

[16] M. Zhao, L. Meng, L. Ma, L. Ma, X. Yang, Y. Huang, J.E. Ryu, A. Shankar, T. Li, C. Yan, others, Layer-by-layer grafting CNTs onto carbon fibers surface for enhancing the interfacial properties of epoxy resin composites, Compos Sci Technol. 154 (2018) 28–36.

[17] B. Wang, S. Ma, X. Xu, Q. Li, T. Yu, S. Wang, S. Yan, Y. Liu, J. Zhu, High-Performance,

Biobased, Degradable Polyurethane Thermoset and Its Application in Readily Recyclable Carbon Fiber Composites, ACS Sustain Chem Eng. 8 (2020) 11162–11170.

[18] S. Tiwari, J. Bijwe, Surface treatment of carbon fibers-a review, Procedia Technol. 14 (2014) 505–512.

[19] F. Gnädinger, P. Middendorf, B. Fox, Interfacial shear strength studies of experimental carbon fibres, novel thermosetting polyurethane and epoxy matrices and bespoke sizing agents, Compos Sci Technol. 133 (2016) 104–110.

[20] Y. Zhang, Y. Zhang, Y. Liu, X. Wang, B. Yang, A novel surface modification of carbon fiber for high-performance thermoplastic polyurethane composites, Appl Surf Sci. 382 (2016) 144–154.

[21] G. Zhao, T. Wang, Q. Wang, Surface modification of carbon fiber and its effects on the mechanical and tribological properties of the polyurethane composites, Polym Compos. 32 (2011) 1726–1733.

[22] R.L. Zhang, Y. Liu, Y.D. Huang, L. Liu, Effect of particle size and distribution of the sizing agent on the carbon fibers surface and interfacial shear strength (IFSS) of its composites, Appl Surf Sci. 287 (2013) 423–427.

[23] Y.D. Huang, R.L. Zhang, L. Liu, D. Su, A method of preparation the waterborne epoxy resin sizing agent for the carbon fiber, Pat CN 2010103001313. (2010).

[24] S.M. Goushegir, J.F. Dos Santos, S.T. Amancio-Filho, Friction spot joining of aluminum AA2024/carbon-fiber reinforced poly (phenylene sulfide) composite single lap joints: microstructure and mechanical performance, Mater Des. 54 (2014) 196–206.

[25] S. Jiang, Q. Li, Y. Zhao, J. Wang, M. Kang, Effect of surface silanization of carbon fiber on mechanical properties of carbon fiber reinforced polyurethane composites, Compos Sci Technol. 110 (2015) 87–94.

[26] P. Yeole, S. Alwekar, N.K.P. Veluswamy, S. Kore, N. Hiremath, U. Vaidya, M. Theodore, Characterization of textile-grade carbon fiber polypropylene composites, Polym Polym Compos.

(2020) 0967391120930109.

[27] M.S. Kathalewar, P.B. Joshi, A.S. Sabnis, V.C. Malshe, Non-isocyanate polyurethanes: from chemistry to applications, RSC Adv. 3 (2013) 4110–4129.

[28] Z. Liu, Y. Tian, S. Kang, X. Zhang, Synthesis and characterization of novel epoxy-modified waterborne polyurethanes and their use in carbon fiber sizing, J Appl Polym Sci. 125 (2012) 3490–3499.

[29] A. ASTM, D4065-01 standard practice for determining and reporting dynamic mechanical properties of plastics, West Conshohocken, PA Am Soc Test Mater. (2001).

[30] A. D7028--15, Standard Test Method for Glass Transition Temperature (DMA Tg) of Polymer Matrix Composites by Dynamic Mechanical Analysis (DMA), (2015).

[31] A. Alten, E. Erzi, Ö. Gürsoy, G.H. A\ugao\uglu, D. Dispinar, G. Orhan, Production and mechanical characterization of Ni-coated carbon fibers reinforced Al-6063 alloy matrix composites, J Alloys Compd. 787 (2019) 543–550.

[32] L.F.M. Da Silva, A. Öchsner, R.D. Adams, Handbook of adhesion technology, Springer Science \& Business Media, 2011.

[33] I. ASTM, Standard test methods for flexural properties of unreinforced and reinforced plastics and electrical insulating materials, ASTM D790-07. (2007).

[34] D. ASTM, Standard test method for apparent interlaminar shear strength of parallel fiber composite by short beam method, Pennsylvania, USA. (2012).

[35] A.A.S. for Testing, Materials, Standard test methods for determining the Izod pendulum impact resistance of plastics, ASTM international, 2010.

[36] Q. Ma, Y. Gu, M. Li, S. Wang, Z. Zhang, Effects of surface treating methods of high-strength carbon fibers on interfacial properties of epoxy resin matrix composite, Appl Surf Sci. 379 (2016) 199–205.

[37] R. Ruan, W. Cao, L. Xu, Quantitative characterization of physical structure on carbon fiber

surface based on image technique, Mater Des. 185 (2020) 108225.

[38] W. Jiao, Y. Cai, W. Liu, F. Yang, L. Jiang, W. Jiao, R. Wang, Preparation of carbon fiber unsaturated sizing agent for enhancing interfacial strength of carbon fiber/vinyl ester resin composite, Appl Surf Sci. 439 (2018) 88–95.

[39] J.C.Q. Amado, Thermal Resistance Properties of Polyurethanes and Its Composites, in: Thermosoftening Plast, IntechOpen, 2019.

[40] F. Wang, M. Yang, S. Zhou, S. Ran, J. Zhang, Effect of fiber volume fraction on the thermal and mechanical behavior of polylactide-based composites incorporating bamboo fibers, J Appl Polym Sci. 135 (2018) 46148.

[41] S. Keusch, R. Haessler, Influence of surface treatment of glass fibres on the dynamic mechanical properties of epoxy resin composites, Compos Part A Appl Sci Manuf. 30 (1999) 997–1002.

[42] D.D. Edie, J.M. Kennedy, R.J. Cano, R.A. Ross, Evaluating surface treatment effects on interfacial bond strength using dynamic mechanical analysis, in: Compos Mater Fatigue Fract Fourth Vol, ASTM International, 1993.

[43] P. Kiss, W. Stadlbauer, C. Burgstaller, V.-M. Archodoulaki, Development of high-performance glass fibre-polypropylene composite laminates: Effect of fibre sizing type and coupling agent concentration on mechanical properties, Compos Part A Appl Sci Manuf. 138 (2020) 106056.

[44] C. Ozkan, N.G. Karsli, A. Aytac, V. Deniz, Short carbon fiber reinforced polycarbonate composites: Effects of different sizing materials, Compos Part B Eng. 62 (2014) 230–235.

[45] F. Schue, Transreactions in condensation polymers, Edited by Stoyko Fakirov. Wiley-VCH, 1999, pp 485, price£140 ISBN 3-527-29790-1, Polym Int. 49 (2000) 806–807.

[46] L.D. Agnol, H.L. Ceratti, D. Favero, S.P. Rempel, L. da S.A. Schiavo, J.R. Ernzen, F.T.G. Dias, O. Bianchi, Transurethanization reaction as an alternative for melt modification of polyamide 6, J Polym Res. 26 (2019) 112.

[47] K.S. Ahmed, S. Vijayarangan, Tensile, flexural and interlaminar shear properties of woven jute

and jute-glass fabric reinforced polyester composites, J Mater Process Technol. 207 (2008) 330–335.

[48] Y. Wang, S.K. Raman Pillai, J. Che, M.B. Chan-Park, High interlaminar shear strength enhancement of carbon fiber/epoxy composite through fiber-and matrix-anchored carbon nanotube networks, ACS Appl Mater Interfaces. 9 (2017) 8960–8966.

[49] Z. Fan, M.H. Santare, S.G. Advani, Interlaminar shear strength of glass fiber reinforced epoxy composites enhanced with multi-walled carbon nanotubes, Compos Part A Appl Sci Manuf. 39 (2008) 540–554.

[50] P.K. Mallick, Fiber-reinforced composites: materials, manufacturing, and design, CRC press, 2007.

[51] T. Yu, J. Ren, S. Li, H. Yuan, Y. Li, Effect of fiber surface-treatments on the properties of poly (lactic acid)/ramie composites, Compos Part A Appl Sci Manuf. 41 (2010) 499–505.

[52] P.H. Thornton, Energy absorption in composite structures, J Compos Mater. 13 (1979) 247–262.

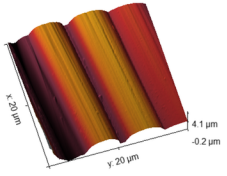

Unsized

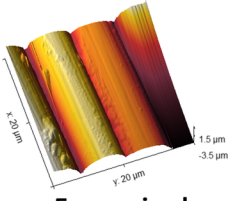

Epoxy sized

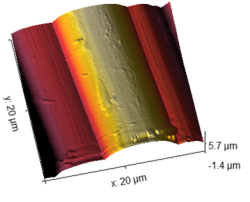

Urethane sized

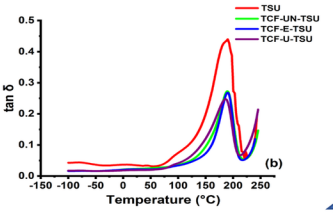

Effect of sizing on TCF-TSU composites

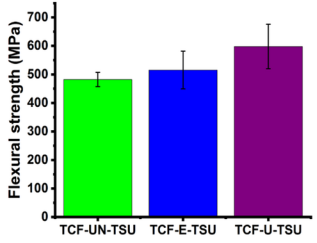

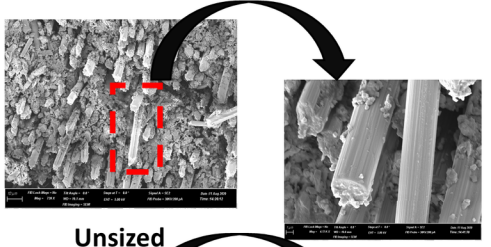

Unsized

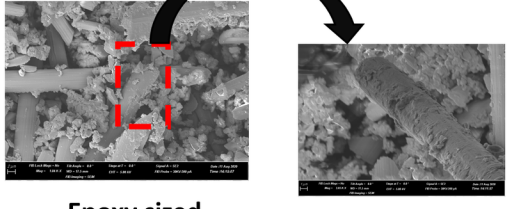

Epoxy sized

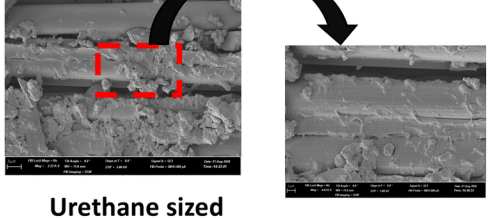

Urethane sized